

## Synthesis and Characterization of Ruthenium polypyridyl complexes for alkene epoxidation catalysis

---

Estudiant: Lorenzo Rico Lazaro

Grau en Química

Correu electrònic: signo7@gmail.com

Tutor: M<sup>a</sup> Isabel Romero

Empresa / institució: Universitat de Girona

Vistiplau tutor:

Nom del tutor: M<sup>a</sup> Isabel Romero

Empresa / institució: Universitat de Girona

Correu(s) electrònic(s): marisa.romero@udg.edu

## Index

AGRAÏMENTS	I
RESUM	II
RESUMEN	III
SUMMARY	IV
GLOSSARY OF TERMS AND ABBREVIATIONS	V
<b>CHAPTER 1. INTRODUCTION</b>	<b>1</b>
1.1 Ruthenium complexes properties	1
1.2 Ruthenium polypyridyl aqua complexes	1
1.3 Ruthenium in epoxidation catalysis of olefins	2
<b>CHAPTER 2. OBJECTIVES</b>	<b>4</b>
<b>CHAPTER 3. EXPERIMENTAL SECTION</b>	<b>5</b>
3.1 Instrumentation and measurements	5
3.2 Synthesis of compounds	6
3.3 Catalytic experiments	9
3.3.1 Conditions of alkene epoxidation	9
3.4 Ethical and sustainability criteria	10
<b>CHAPTER 4. RESULTS AND DISCUSSION</b>	<b>11</b>
4.1 Synthesis and structural characterization	11
4.2 Spectroscopic properties	16
4.2.1 IR spectroscopy	16
4.2.2 NMR spectroscopy	17
4.2.3 UV-Vis spectroscopy	19
4.3 Electrochemical properties	19
4.4 Catalytic epoxidation reactions	23
<b>CHAPTER 5. CONCLUSIONS</b>	<b>25</b>
<b>CHAPTER 6. BIBLIOGRAPHY</b>	<b>27</b>

## **AGRAÏMENTS**

A la Doctora Marisa Romero, tutora del treball de fi de grau, per la seva exigència, orientació i la confiança d'acompanyar-me durant la trajectòria del projecte. Gràcies al conjunt de l'equip de recerca, Catàlisi i Sostenibilitat, en especial a l'Ester Manrique per la seva dedicació i el seu continu suport en tot moment del projecte. Gràcies als altres estudiants de treball de final de grau, companys de classe i a l'hora amics per fer que les moltes hores de laboratori i de despatx fossin més amenes.

## RESUM

En aquest treball de final de grau s'ha desenvolupat i optimitzat una ruta sintètica per obtenir diferents complexos de ruteni amb lligands tipus N-donors, posteriorment s'ha avaluat l'eficiència d'un aquo complex com a catalitzador per a l'epoxidació d'alquens.

Inicialment, s'ha sintetitzat un dels lligands N-donors no comercial (pypz-H) seguidament, s'ha sintetitzat el producte de partida *cis,cis*-[RuCl<sub>2</sub>(dmsu)<sub>2</sub>(pypz-H)] **2**, seguidament aquest complex mononuclear reacciona amb el lligand trpy per generar una mescla del cloro complex *cis* i *trans*-[RuCl(trpy)(pypz-H)](PF<sub>6</sub>) **3b** i **3a**, aquests isòmers han pogut ser separats mitjançant cristal·lització i columna cromatogràfica. Posteriorment a partir d'aquest cloro complex s'ha sintetitzat i caracteritzat l'aquo-complex *trans*-[Ru(trpy)(pypz-H)(OH<sub>2</sub>)](PF<sub>6</sub>)<sub>2</sub> **4a**.

Tots els compostos han sigut caracteritzats mitjançant tècniques espectroscòpiques en dissolució (RMN, UV-Visible) i alguns d'ells mitjançant difracció de Raig X, corroborant que mantenen la seva estructura en estat sòlid.

Les propietats redox dels compostos han sigut estudiades mitjançant CV i DPV. El diagrama de Pourbaix presentat per el compost *trans*-[Ru(trpy)(pypz-H)(OH<sub>2</sub>)](PF<sub>6</sub>)<sub>2</sub> **4a** ha permès obtenir informació dels equilibris redox així com també s'ha pogut conèixer els corresponents valors de pKa de les espècies de Ru<sup>II</sup> i Ru<sup>III</sup>.

Per acabar, s'ha avaluat l'activitat catalítica del complex *trans*-[Ru(trpy)(pypz-H)(OH<sub>2</sub>)](PF<sub>6</sub>)<sub>2</sub> **4a** en l'epoxidació d'alquens, utilitzant PhI(OAc)<sub>2</sub> com a oxidant. Els resultats han mostrat bones conversions pels compostos provats amb uns excel·lents valors de selectivitat.

## RESUMEN

En este trabajo de final de grado se ha desarrollado y optimizado una ruta sintética para obtener diferentes complejos de rutenio con ligandos tipo N-dadores, posteriormente se ha evaluado la eficiencia de un aquo complejo como catalizador en la epoxidación de alquenos.

Inicialmente se ha sintetizado uno de los ligandos N-dadores no comercial (pypz-H), así como el producto de partida *cis,cis*-[RuCl<sub>2</sub>(dms<sub>o</sub>)<sub>2</sub>(pypz-H)] **2**, seguidamente este complejo mononuclear reacciona con el ligando trpy para generar una mezcla del cloro complejo *cis, trans*-[RuCl(trpy)(pypz-H)](PF<sub>6</sub>) **3b** y **3a**, cuyos isómeros han podido ser separados a través de cristalización y columna de cromatografía. Posteriormente a partir de este cloro-complejo se ha sintetizado y caracterizado el aquo complejo, *trans*-[Ru(trpy)(pypz-H)(OH<sub>2</sub>)](PF<sub>6</sub>)<sub>2</sub> **4a**.

Todos los compuestos se han caracterizado mediante técnicas espectroscópicas en disolución (RMN, UV-Visible) y algunos de ellos mediante difracción de Rayos X, corroborando que mantienen su estructura en estado sólido.

Las propiedades redox de los compuestos han sido estudiadas mediante CV y DPV. El diagrama de Pourbaix presentado por el compuesto *trans*-[Ru(trpy)(pypz-H)(OH<sub>2</sub>)](PF<sub>6</sub>)<sub>2</sub> **4a** ha permitido obtener información de los equilibrios redox así como también se ha podido conocer los correspondientes valores de pKa de las especies de Ru<sup>II</sup> y Ru<sup>III</sup>.

Finalmente, se ha comprobado la actividad catalítica del complejo *trans*-[Ru(trpy)(pypz-H)(OH<sub>2</sub>)](PF<sub>6</sub>)<sub>2</sub> **4a** en la epoxidación de alquenos, utilizando PhI(OAc)<sub>2</sub> como oxidante. Los resultados obtenidos han mostrado buenas conversiones para los compuestos probados así como excelentes valores de selectividad.

## SUMMARY

In this dissertation work we have developed and optimized a synthetic route to obtain different ruthenium complexes with N-donor type ligands, afterwards, we have evaluated the efficiency of an aqua-complex as catalyst for the epoxidation of alkenes.

Initially we have synthesized one of the non-commercial N-donor ligand (pypz-H), and the starting product *cis,cis*-[RuCl<sub>2</sub>(dmsO)<sub>2</sub>(pypz-H)] **2**, this mononuclear complex reacts further with the ligand trpy to generate a mixture of the chloro-complex *cis, trans*-[RuCl(trpy)(pypz-H)](PF<sub>6</sub>) **3b** and **3a**. Afterwards, from this one we have synthesized and characterized the correspondent aqua-complex *trans*-[Ru(trpy)(pypz-H)(OH<sub>2</sub>)](PF<sub>6</sub>)<sub>2</sub> **4a**.

All the compounds have been characterized in solution through spectroscopic techniques (RMN, UV-Visible) and some of them by X-ray diffraction, confirming that they maintain their structure in solid state.

The redox properties of the compounds have been studied by CV and DPV. The Pourbaix diagram displayed by the complex *trans*-[Ru(trpy)(pypz-H)(OH<sub>2</sub>)](PF<sub>6</sub>)<sub>2</sub> **4a** allowed to obtain data about the redox equilibriums as well as have allowed to know the correspondent pKa values of the Ru<sup>II</sup> and Ru<sup>III</sup> species.

Finally, we have evaluated the catalytic activity of the complex *trans*-[Ru(trpy)(pypz-H)(OH<sub>2</sub>)](PF<sub>6</sub>)<sub>2</sub> **4a** in the alkene epoxidation, using PhI(OAc)<sub>2</sub> as oxidant. The results obtained shown good conversion values for the compounds tested as well as excellent selectivity values.

## GLOSSARY OF TERMS AND ABBREVIATIONS

Abs	Absorbance
abs.	Absolute
acetone-d <sub>6</sub>	Deuterated acetone
Anal. Found (Calc.)	Analysis found (analysis calculated)
trpy	2,2';6',2''-terpyridine
bpy	2,2'-bipyridine
Cl	Chloride
CDCl <sub>3</sub>	Deuterated chloroform
CV	Cyclic voltammetry
d	Doublet
dmsO	Dimethyl sulfoxide
ε	Extinction coefficient
E	Potential
E <sub>1/2</sub>	Half-wave potential
ESI-MS	Electrospray ionization mass spectrometry
ET	Electron transfer
h	Hours
IR	Infrared
J	Coupling constant
M	Metal
m	Multiplet
MHz	Megahertz
MLCT	Metal to ligand charge transfer
MeOH	Methanol
Methanol-d <sub>4</sub>	Deuterated methanol
m/z	Mass-to-charge ratio
NMR	Nuclear magnetic resonance
PCET	Proton-coupled-electron transfer
ppm	Parts per million
pypz-H	2-(3-pyrazolyl)pyridine
pypz-Me	2-(1-Methyl-3-pyrazolyl)pyridine
S	Sulfur
s	Singlet
Ru	Ruthenium
RT	Room Temperature
T	Temperature
t	Triplet
TBAH	Tetra(n-butyl)ammonium hexafluorophosphate
TON	Turnover number
UV-Vis	Ultraviolet-visible spectroscopy
vs	Versus
λ	Wavelength
δ	Chemical shift

## CHAPTER 1. INTRODUCTION

### 1.1 Ruthenium complexes properties

Ruthenium is a metal situated in the d group of the periodic table. The electronic configuration of ruthenium ( $[\text{Kr}] 4d^7 5s^1$ ) makes this metal, together with osmium, unique among most of the elements in displaying the widest range of oxidation states in their complexes. The oxidation state of ruthenium takes place from -2 as in  $[\text{Ru}(\text{CO})_2]^{2+}$  ( $d^0$ ) to +8 as in  $\text{RuO}_4$  ( $d^{10}$ ). The synthetic versatility and the kinetic stability of ruthenium complexes in different oxidation states make these complexes particularly interesting. Other characteristics of ruthenium's coordination compounds are their high electron transfer capacity,<sup>1</sup> a robust character of their coordination sphere, their redox-active capacity, their easily available high oxidation states and their applications as redox reagents in many different chemical reactions.

Ruthenium complexes have experienced a large boost in the fields of catalysis,<sup>2</sup> photochemistry and photophysics,<sup>3</sup> and more recently in supramolecular<sup>4</sup> and bio-inorganic chemistry.<sup>5</sup>

The properties of ruthenium complexes are certainly correlated with the nature of the ligands coordinated to the central metal ion. Ruthenium complexes with N-donor ligands are studied due to their spectroscopic, photophysical and electrochemical properties.<sup>6</sup> On the other hand, ruthenium complexes with  $\pi$ -conjugate ligands or systems that enable electronic delocalization have shown specific properties in nonlinear optics, magnetism, molecular sensors and liquid crystals.<sup>7</sup> Furthermore, ruthenium complexes with heterocyclic N-donor ligands are the most used due to their interesting spectroscopic, photophysical and electrochemical properties.<sup>8</sup>

### 1.2 Ruthenium polypyridyl aqua complexes

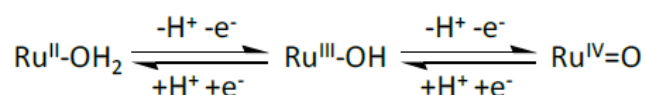
In recent years, the study on ruthenium complexes with N-donor ligands have received much attention owing to their interesting uses in diverse areas such as photo sensitizers, as oxidation catalysis<sup>9</sup>, for photochemical conversion of solar energy,<sup>10</sup> molecular electronic devices<sup>11</sup> and photoactive DNA cleavage agents for therapeutic purposes.<sup>12</sup>



Extensive coordination chemistry about hexacoordinated complexes containing polypyridyl ligands has been reported, due to the stability of these ligands against oxidation and their great coordinative capacity, increased by their quelating effect. These properties give a great stability to the formed complex.

The redox properties of these complexes become especially interesting when an aqua ligand is directly bonded to the metal center. In this case, a proton-coupled-electron transfer (PCET) is possible, making the high oxidation states fairly accessible.<sup>13</sup>

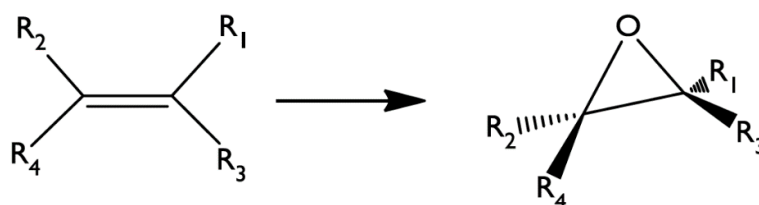
The successive oxidation from Ru(II) to Ru(IV) are accompanied by a sequential loss of protons favored by the enhanced acidity of the bonded aqua ligand (*Scheme 1*). Therefore, the initial Ru<sup>II</sup>-OH<sub>2</sub> is oxidized to Ru<sup>IV</sup>=O, passing through a Ru<sup>III</sup>-OH species.



**Scheme 1.** PCET oxidation process characteristic of Ru-aqua complexes.

### 1.3 Ruthenium in epoxidation catalysis of olefins

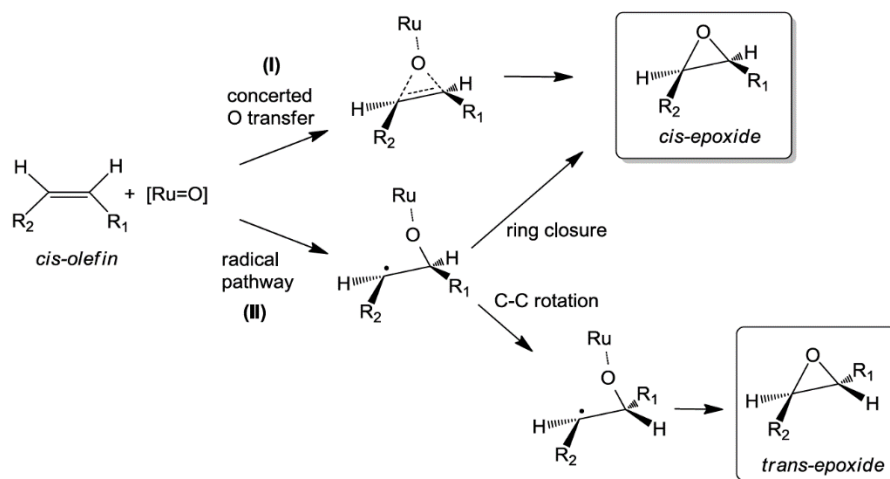
The catalytic epoxidation of alkenes (*Scheme 2*) has great importance from academics and industry point of view. Olefin epoxidation has an interest due to the fact that epoxides are useful as intermediates in organic reactions and they can be easily transformed to functionalized compounds.<sup>14</sup> Epoxides are used in the synthesis of many industrial products, for example, in fine chemical some anti-inflammatory and anti-allergic agents are synthesized from epoxides.<sup>15</sup> Epoxy polymers are widely used in the marine, automotive, aerospace and building industries.



**Scheme 2.** Alkene epoxidation process.

Ruthenium complexes have been proved to be efficient in the epoxidation of different olefins with relatively high selectivities.<sup>16</sup> In general, epoxide yields depend on several factors such as the nature of the substrates, catalysts and reaction conditions.

A key point in ruthenium-mediated epoxidation is the mechanism followed.<sup>17</sup> Two general routes have been described, which are depicted in Scheme 3 for a general *cis*-olefin:



**Scheme 3.** Possible pathways for metal-catalyzed epoxidation.

The concerted oxo transfer (I) leads to a *stereospecific* epoxidation, keeping the *cis* stereoisomerism of the original alkene in the final epoxide product, whereas the radical pathway (II) generates an intermediate specie that can either undergo direct ring closure (also leading to the *cis*-epoxide) or, alternatively, it can suffer C-C bond rotation prior to ring closure leading to the *trans*-epoxide, which is thermodynamically more stable. Depending on the relative reaction rates of these processes, the radical mechanism can result in a mixture of *cis*- and *trans*-epoxides.

## CHAPTER 2. OBJECTIVES

The aims of this work are the ones following:

- To learn the techniques of synthesis and spectroscopic and electrochemical characterization, which are characteristic of a research laboratory.
- The synthesis of new ruthenium (II) complexes (chloro and aqua), containing polypyridylic ligands. The ligands used in this work are the ones following in the *Figure 1*.

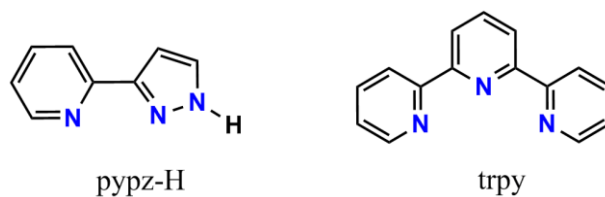


**Figure 1.** Plot for ligands used in this work

- The spectroscopic and electrochemical characterization of the complexes synthesized.
- The evaluation of the synthesized complex  $\text{trans-}[\text{Ru}^{\text{II}}(\text{H}_2\text{O})(\text{pypz-H})(\text{trpy})](\text{PF}_6)_2$  **4a** in the catalytic epoxidation of alkenes.

## CHAPTER 3. EXPERIMENTAL SECTION

### 3.1 Instrumentation and measurements

- *UV-Vis*

UV-Vis spectroscopy was performed on a Cary 50 Scan (Varian) UV-Vis spectrophotometer with 1 cm quartz cells.

- *Cyclic voltammetry (CV) and differential pulse voltammetry (DPV)*

CV and DPV experiments were performed in an IJ-Cambria IH-660 potentiostat using a three electrode cell. Glassy carbon electrode (3 mm diameter) from BAS was used as working electrode, platinum wire as auxiliary and SCE as the reference electrode. The complexes were dissolved in solvents containing the necessary amount of  $n\text{-Bu}_4\text{NPF}_6$  (TBAH) as supporting electrolyte to yield a 0.1 M ionic strength solution. All  $E_{1/2}$  values reported in this work were estimated from cyclic voltammetry experiments as the average of the oxidative and reductive peak potentials  $(E_{p,a}+E_{p,c})/2$ , or directly from DPV peaks.

- *IR*

IR spectroscopy was performed on an Agilent Technologies, Cary 630 FTIR equipped with an ATR system, directly on the samples without any previous treatment.

- *NMR spectra*

The NMR spectroscopy was performed on a Bruker DPX 400 MHz. Samples were run in  $\text{CD}_2\text{Cl}_2$ ,  $\text{CDCl}_3$ ,  $\text{CD}_3\text{OD}$  and  $(\text{CD}_3\text{OD}/10\% \text{CF}_3\text{COOD})$ . For the NMR assignments, we used the same labeling scheme as for the X-ray structures.

- *Gas chromatography*

Gas chromatography experiments were performed by capillary GC, using a GC-2010 Gas Chromatograph from Shimadzu, equipped with an Astec CHIRALDEX G-TA Column (30 m x 0.25 mm diameter) incorporating a FID detector. All the product analyses in the catalytic experiments were performed by means of calibration curves using biphenyl as internal standard. GC conditions: initial temperature, 40° C for 5 min; ramp rate, 5° C min<sup>-1</sup>; final temperature, 170 °C; injection temperature, 250 °C, detector temperature, 250 °C, carrier gas, He at 25 mL min<sup>-1</sup>.

- *X-ray Structure Determination*

The measurement was carried out on a *BRUKER SMART APEX CCD* diffractometer using graphite-monochromated Mo  $K\alpha$  radiation ( $\lambda = 0.71073 \text{ \AA}$ ) from an x-Ray Tube. The measurements were made in the range 2.461 to 28.426° for  $\theta$ . Full-sphere data collection was carried out with  $\omega$  and  $\varphi$  scans. A total of 21219 reflections were collected of which 7288 [ $R(\text{int}) = 0.0458$ ] were unique. Programs used: data collection, Smart<sup>18</sup>; data reduction, Saint+<sup>19</sup>; absorption correction, SADABS<sup>20</sup>. Structure solution and refinement was done using SHELXT and SHELXL<sup>21</sup>.

The structure was solved by direct methods and refined by full-matrix least-squares methods on  $F^2$ . The non-hydrogen atoms were refined anisotropically. The H-atoms were placed in geometrically optimized positions and forced to ride on the atom to which they are attached, except for the N-H hydrogen which was refined freely.

### 3.2 Synthesis of compounds

**Materials.** All reagents used in the present work were obtained from Aldrich Chemical Co. in the highest commercially available purity grade and were used without further purification. Reagent grade organic solvents were obtained from SDS and high purity deionized water was obtained by passing distilled water through a nanopore Mili-Q water purification system.

**Synthesis.** Ligand [3-(2-pyridyl)pyrazole] pypz-H<sup>22</sup> and complexes *cis*-[Ru<sup>II</sup>Cl<sub>2</sub>(dms<sub>2</sub>)<sub>4</sub>] **1**<sup>23</sup>, *cis*, *cis*-[Ru<sup>II</sup>Cl<sub>2</sub>(pypz-H)(dms<sub>2</sub>)<sub>2</sub>] **2**<sup>24</sup> were prepared as described in the literature. All synthetic manipulations were routinely performed under nitrogen atmosphere using Schlenk tubes and vacuum line techniques.

#### Synthesis of the ligand 2-(3-pyrazolyl)pyridine, pypz-H

1 g (5.67 mmol) of 3-(dimethylamino)-1-(2-pyridyl)-2-propen-1-one together with 0.4 mL (7.42 mmol) of hydrazine were refluxed in ethanol (20 mL) at 110°C for 1 hour. The mixture was cooled to room temperature. Once cooled, the solvent was evaporated in a vacuum. The brown precipitated correspond to pypz-H. Yield: 0.81 g (99%). <sup>1</sup>H-NMR (400 MHz, CDCl<sub>3</sub>):  $\delta$ = 6.81 (d, 1H, H5), 7.23 (dd, 1H, H4), 7.66 (d, 1H, H6), 7.74 (ddd, 2H, H2, H3), 8.63 (dd, 1H, H1).

**Synthesis of [RuCl<sub>2</sub>(dmsO)<sub>4</sub>], 1**

1g (3.83 mmol) of RuCl<sub>3</sub>·2.53H<sub>2</sub>O was refluxed in 5 mL of dmsO at 150 °C for 30 minutes. After this time, the solution was cooled to RT; 50 mL of acetone were added. The yellow precipitate formed was separated by filtration and successively washed with acetone and ether and dried in vacuum. Yield: 1.095 g (57%).

**Synthesis of *cis,cis*-[Ru<sup>II</sup>Cl<sub>2</sub>(pypz-H)(dmsO)<sub>2</sub>], 2**

A mixture of [RuCl<sub>2</sub>(dmsO)<sub>4</sub>] **1** (250 mg, 0.51 mmol), and pypz-H (75 mg, 0.52 mmol) was dissolved in 50 mL of ethanol absolute and heated at 90°C under nitrogen atmosphere for 2 hours. After the reaction time, the solution was cooled to room temperature and the volume was reduced in a rotary evaporator. The yellow precipitate formed (corresponds to compound **2**) was separated by filtration and successively washed with ether and dried in vacuum. Yield: 179 mg (58%). <sup>1</sup>H-NMR (400 MHz, CD<sub>2</sub>Cl<sub>2</sub>): δ = 2.00 (s, 3H, H11), 2.92 (s, 3H, H10), 3.52 (s, 3H, H9), 3.54 (s, 3H, H8), 6.99 (d, 1H, H5, J<sub>5,6</sub>=2.8Hz), 7.54 (ddd, 1H, H2, J<sub>2,1</sub>=6.8Hz; J<sub>2,3</sub>=7.4Hz; J<sub>2,4</sub>=1.5Hz), 7.79 (d, 1H, H6, J<sub>6,5</sub>=2.8Hz), 7.95 (ddd, 1H, H4, J<sub>4,3</sub>=7.4Hz; J<sub>4,2</sub>=1.5Hz; J<sub>4,1</sub>=0.9Hz), 8.02 (td, 1H, H3, J<sub>3,2</sub>=J<sub>3,4</sub>=7.4Hz; J<sub>3,1</sub>=1.5Hz), 9.44 (ddd, 1H, H1, J<sub>1,2</sub>=6.8Hz; J<sub>1,3</sub>=1.5Hz; J<sub>1,4</sub>=0.9Hz), 13.11 ppm(s, 1H, H7). E<sub>1/2</sub><sup>(III/II)</sup> (CH<sub>2</sub>Cl<sub>2</sub> + 0.1 M TBAH): 1.12 V vs. SCE.

**Synthesis of *trans*- and *cis*-[Ru<sup>II</sup>Cl(pypz-H)(trpy)](PF<sub>6</sub>), 3a and 3b**

0.558 g (1.179 mmol) of [Ru<sup>II</sup>Cl<sub>2</sub>(dmsO)(pypz-H)] **2**, complex and 0.275 g (1.155 mmol) of trpy were refluxed in 150 mL of methanol for 18 h. The dark reaction mixture was reduced to dryness and redissolved in 10 mL of a 75:1 mixture of MeOH/NH<sub>4</sub>OH. The mixture was cooled until a brown precipitate P1 was formed. This solid was filtered on a frit and washed two times with cold MeOH/NH<sub>4</sub>OH (75:1) solution. The filtrate solution, F1 which contained mainly the *cis*-isomer, was reduced to 5 mL volume and purified by column chromatography (vide infra). The P1 was dissolved with a mixture of MeOH/HCl (adjusting the pH to < 2) and a 1 mL of a saturated aqueous solution of NH<sub>4</sub>PF<sub>6</sub> was added. Afterwards 100 mL of cold water was added under vigorous stirring. The pure **3a** complex was obtained as a precipitate, was filtered off and washed with cold H<sub>2</sub>O and diethyl ether. Yield: 0.267 g (34%).

Suitable crystals of **3a** were grown as brownish-purple needles by diffusion of diethyl ether into a CH<sub>2</sub>Cl<sub>2</sub> solution of the pure complex.

Column chromatography on silica was carried out (SiO<sub>2</sub>, MeOH/NH<sub>4</sub>OH 30:1), the first yellow fraction was discarded and contained Ru(trpy)<sub>2</sub><sup>2+</sup>. A second purple fraction contained a small amount of the **3a** isomer which one was also discarded. Finally, a third brownish fraction contained the **3b** was obtained. The volume of the later fraction was reduced to dryness and dissolved with 10 mL of a mixture of MeOH/HCl (adjusting the pH to < 2), then 1 mL of saturated aqueous NH<sub>4</sub>PF<sub>6</sub> solution was added. Finally 100 mL of water was added under vigorous stirring and cooling until precipitation. The fine crystalline precipitate was filtered off, washed twice with 10 mL of water and 10 mL of diethyl ether. and dried in vacuum. Yield: 98.7 mg (13 %) of pure **3b** complex was obtained.

For **3a**: **<sup>1</sup>H NMR (400 MHz, Methanol-d<sub>4</sub>)**: δ 10.03 (ddd, *J* = 5.7, 1.4, 0.9 Hz, 1H, H1), 8.59 (d, *J* = 8.1 Hz, 2H, H15, H17), 8.48 (d, *J* = 8.1 Hz, 2H, H12, H20), 8.37 (d, *J* = 7.7 Hz, 1H, H4), 8.23 (td, *J* = 7.8, 1.5 Hz, 1H, H3), 8.11 (t, *J* = 8.1 Hz, 1H, H16), 7.92 (td, *J* = 7.8, 1.5 Hz, 2H, H11, H21), 7.83 (td, *J* = 5.7, 1.4 Hz, 1H, H2), 7.71 (ddd, *J* = 5.5, 1.4, 0.7 Hz, 2H, H9, H23), 7.48 (d, *J* = 2.8 Hz, 1H, H8), 7.33 (ddd, *J* = 7.5, 5.5, 1.3 Hz, 2H, H10, H22), 7.10 ppm(d, *J* = 2.8 Hz, 1H, H7). **<sup>13</sup>C NMR (400 MHz, Methanol-d<sub>4</sub>)**: δ 158.8 (C14, C18), 152.6 (C6), 152.1 (C9, C23), 137.2 (C3), 136.6 (C11, C21), 133.3 (C16), 133.0 (C8), 127.2 (C13, C19), 126.8 (C10, C22), 124.2 (C2), 122.8 (C12, C22), 121.9 (C4), 121.8 (C15, C17), 121.3 (C5), 103.9 ppm(C7). **IR (v max, cm<sup>-1</sup>)**: 3626, 3562, 1628, 1445, 1386, 1062, 842, 760. **E<sub>1/2</sub><sup>(III/II)</sup>** (CH<sub>2</sub>Cl<sub>2</sub> + 0.1 M TBAH): 0.80 V vs. SCE. **UV-vis** (CH<sub>2</sub>Cl<sub>2</sub>) [λ<sub>max</sub>, nm (ε, M<sup>-1</sup> cm<sup>-1</sup>)]: 236 (1477), 276 (1235), 322 (1146).

For **3b**: **<sup>1</sup>H-NMR (400 MHz, Methanol-d<sub>4</sub>)**: δ 8.65 (d, *J* = 8.1 Hz, 2H, H15, H17), 8.53 (d, *J* = 8.1 Hz, 2H, H12, H20), 8.41 (d, *J* = 2.9 Hz, 1H, H7), 8.16 (t, *J* = 8.1 Hz, 1H, H16), 8.11 (ddd, *J* = 8.0, 1.5, 1.0 Hz, 1H, H4), 7.95 (td, *J* = 7.9, 1.5 Hz, 2H, H11, H21), 7.79 (ddd, *J* = 5.5, 1.4, 0.7 Hz, 2H, H9, H23), 7.68 (td, *J* = 7.8, 1.4 Hz, 1H, H3), 7.55 (d, *J* = 2.9 Hz, 1H, H8), 7.40 (ddd, *J* = 7.5, 5.6, 1.3 Hz, 2H, H10, H22), 7.18 (ddd, *J* = 5.7, 1.3, 0.8 Hz, 1H, H1), 6.91 ppm(ddd, *J* = 7.4, 5.8, 1.5 Hz, 1H, H2). **<sup>13</sup>C NMR (400 MHz, Methanol-d<sub>4</sub>)**: δ 141.81 (C9, C23), 139.62 (C1), 125.74 (C11, C21), 124.93 (C3), 122.89 (C16), 122.05 (C7), 116.11 (C10, C22), 113.45 (C2), 112.85 (C12, C20), 111.89 (C15, C17), 111.80 (C4), 94.21 ppm(C8). **IR (v max, cm<sup>-1</sup>)**: 3648, 3562, 1594, 1445, 1382, 838, 760. **E<sub>1/2</sub><sup>(III/II)</sup>** (CH<sub>2</sub>Cl<sub>2</sub> + 0.1 M TBAH): 0.88 V vs. SCE. **UV-vis** (CH<sub>2</sub>Cl<sub>2</sub>) [λ<sub>max</sub>, nm (ε, M<sup>-1</sup> cm<sup>-1</sup>)]: 238 (1480), 276 (1163), 318 (1198).

### Synthesis of *trans*-[Ru<sup>II</sup>(H<sub>2</sub>O)(pypz-H)(trpy)](PF<sub>6</sub>)<sub>2</sub>, **4a**

A Sample of AgPF<sub>6</sub> (0.08 g, 0.32 mmol) was added to a solution of 30 mL of H<sub>2</sub>O containing **3a** (0.1 g, 0.15 mmol) and heated at reflux for 2 h in the absence of light. AgCl was filtered off through a frit containing Celite. Afterwards, NH<sub>4</sub>PF<sub>6</sub> (1 mL) was added to the filtrate, and the volume reduced in a rotary evaporator until a precipitate appeared that was washed with the minimum amount of cold water and diethyl ether. Yield: 0.040 g (40%).

For **4a**: <sup>1</sup>H NMR (400 MHz, Methanol-*d*<sub>4</sub>): δ 9.41 (ddd, *J* = 5.6, 1.4, 0.8 Hz, 1H, H1), 8.68 (d, *J* = 8.1 Hz, 2H, H15, H17), 8.56 (d, *J* = 7.9 Hz, 2H, H12, H20), 8.41 (d, *J* = 7.9 Hz, 1H, H4), 8.34 – 8.28 (m, 1H, H3), 8.27 – 8.22 (m, 1H, H16), 8.06 – 7.99 (m, 2H, H11, H21), 7.92 (ddd, *J* = 7.6, 5.7, 1.4 Hz, 1H, H2), 7.78 (ddd, *J* = 5.4, 1.4, 0.7 Hz, 2H, H9, H23), 7.47 (d, *J* = 2.9 Hz, 1H, H7), 7.42 (ddd, *J* = 7.6, 5.5, 1.3 Hz, 2H, H10, H22), 7.09 ppm(d, *J* = 2.9 Hz, 1H, H8). IR (ν max, cm<sup>-1</sup>): 3618, 3551, 1992, 1602, 1449, 820, 756. E<sub>1/2</sub><sup>(III/II)</sup> (phosphate buffer pH=7): 0.26 V vs. SCE. E<sub>1/2</sub><sup>(IV/III)</sup> (phosphate buffer pH=7): 0.65 V vs. SCE. UV-vis (phosphate buffer pH=7): [λ<sub>max</sub>, nm (ε, M<sup>-1</sup> cm<sup>-1</sup>): 230 (18800), 270 (16180), 315 (15060), 381 (3410), 460 (3654).

### Synthesis of *cis*-[Ru<sup>II</sup>(H<sub>2</sub>O)(pypz-H)(trpy)](PF<sub>6</sub>)<sub>2</sub>, **4b**

A Sample of AgPF<sub>6</sub> (0.06 g, 0.24 mmol) was added to a solution of 25 mL of H<sub>2</sub>O containing **3b** (0.08 g, 0.12 mmol) and heated at reflux for 2h. AgCl was filtered off through a frit containing Celite. Afterward NH<sub>4</sub>PF<sub>6</sub> (1 mL) was added to the filtrate, and the volume reduced in a rotary evaporator until a precipitate appeared that was washed with the minimum amount of cold water and ether.

## 3.3 Catalytic experiments

### 3.3.1 Conditions of alkene epoxidation

Experiments have been performed in anhydrous dichloromethane at room temperature. In a typical run, Ru catalyst (0.5 mM), alkene (50 mM), and PhI(OAc)<sub>2</sub> (100 mM) were stirred at room temperature in dichloromethane (2,5 mL) for 24h. After the addition of an internal standard, an aliquot was taken for gas chromatographic (GC) analysis. The oxidized products were analyzed by GC.



### **3.4 Ethical and sustainability criteria**

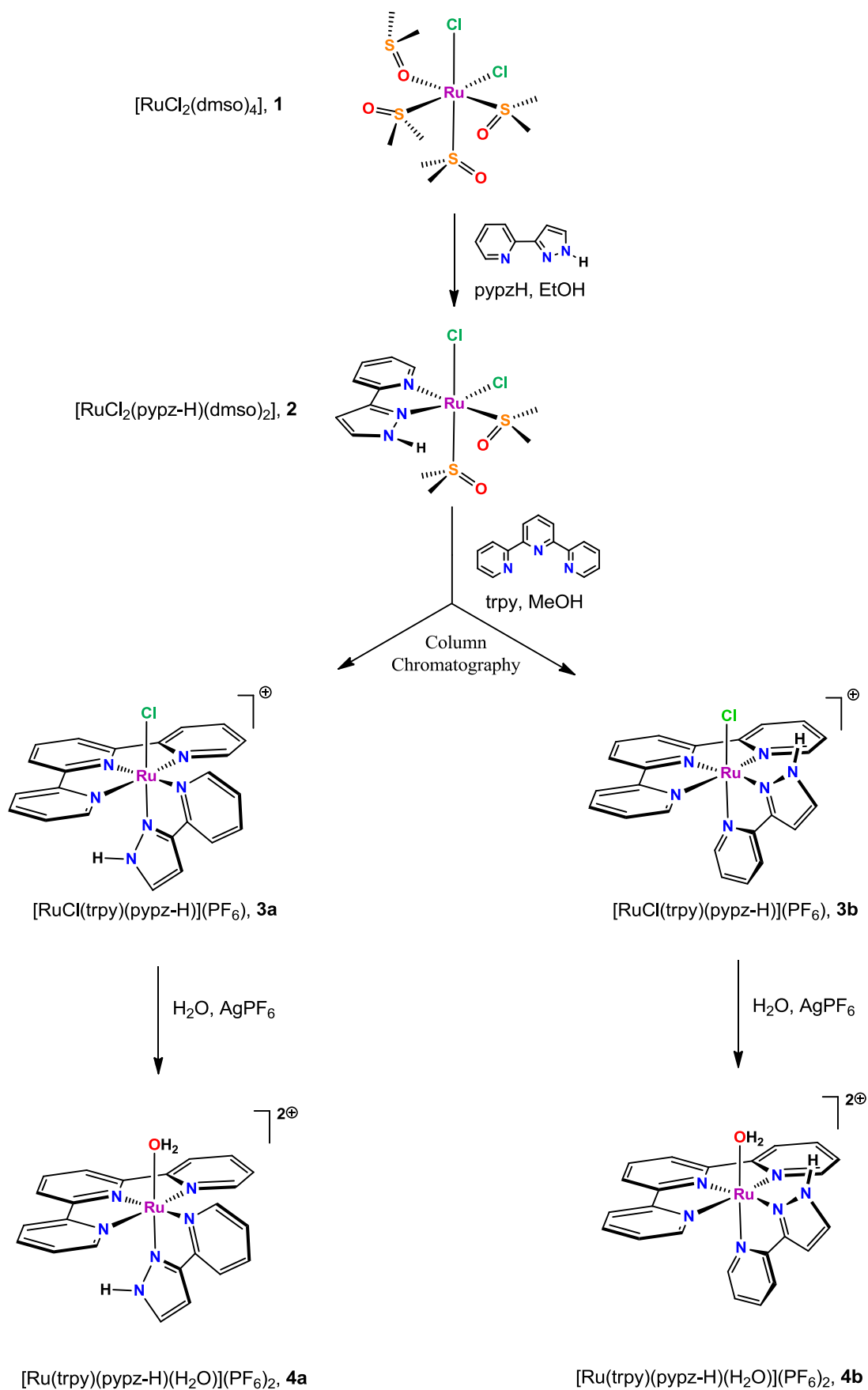
Due to the experimental processes carried out in a synthetic laboratory, sometimes large quantities of solvent were needed, especially in processes of purification of products. However, the waste generated residues were stored properly, in containers intended for properly labeled purpose. It has been tried to work maximizing the atomic economy, but sometimes it has not been possible because the reactions gave some byproducts.

It is worth mentioning that the catalytic study in this work reduces the thermal energy needed for epoxidation reactions, as a clean and economical way to reduce the environmental impact caused by the huge industrial production involved in epoxidation.

## CHAPTER 4. RESULTS AND DISCUSSION

### 4.1 Synthesis and structural characterization

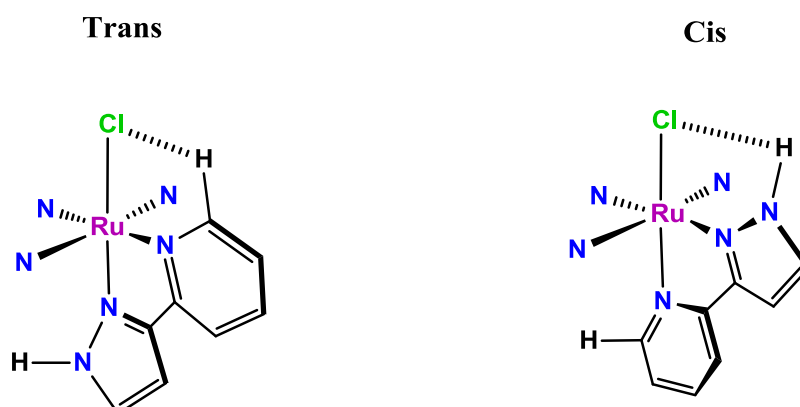
The synthetic strategies followed for the preparation of the Ru(II) complex **4a** and **4b**, is outlined in Scheme 4. The reaction of  $[\text{Ru}^{\text{II}}\text{Cl}_2(\text{dmsO})_4]$  **1** with pypz-H ligand generates the mononuclear complex  $\text{cis}(\text{Cl}),\text{cis}(\text{S})\text{-Ru}^{\text{II}}\text{Cl}_2(\text{pypz-H})(\text{dmsO})_2$ , **2**. This mononuclear complex reacts further with the ligand trpy to generate a mixture of Ru<sup>II</sup>-Cl isomeric complexes, *trans* and *cis*- $[\text{Ru}^{\text{II}}\text{Cl}(\text{trpy})(\text{pypz-H})](\text{PF}_6)$ , **3a** and **3b** with a 4:1 ratio, which are separated and purified through crystallization and column chromatography in silica. Treatment of the corresponding Ru-Cl complex with Ag<sup>+</sup> generates the corresponding aqua ruthenium complexes, **4a** and **4b**. The nomenclature *trans* and *cis* for complexes refers to the relative position of the monodentate ligand with regard to the pyrazole ring of the pypz-H ligand.



**Scheme 4.** Synthetic strategies and ligands used in this work.

The isomer *trans* is favored versus the *cis*, this fact is due probably to steric and electronic effects. In the case of isomer *trans* the steric hindrance is due to the proximity of the pyrazolic proton to the trpy ligand and in the case of the isomer *cis* to the proximity of the pyridilic proton, leading to less steric hindrance in the former case (see scheme 5). Moreover, the isomer *trans* is favored due to the formation of a hydrogen bond between the monodentate chloride ligand Cl1 and H1 of pyridine ring (2.788A) that in the case of isomer *cis* we could assert that would be very weak (see scheme 4). This evidence can be also corroborated by the  $^1\text{H-NMR}$  spectra that in the case of *trans* isomer a strong downfield shift for the pyridilic proton next to the chloride ligand is observed for with regard to the *cis*.

Moreover, the synthetic process also leads to the formation of side products, such as a dimeric specie that is shown below. This fact, could indicate the decrease in the obtention of the *cis* isomer.



**Scheme 5.** Schematic drawing of the *trans* and *cis*- $\text{Ru}^{\text{II}}\text{Cl}(\text{trpy})(\text{pypz-H})](\text{PF}_6)$  complexes indicating the Cl-H interaction.

Crystal structure of isomer *trans*- has been solved by X-ray diffraction analysis. Figure 2 displays the molecular structure whereas the main crystallographic data and selected bond distances and angles can be found in the Tables 1 and 2.

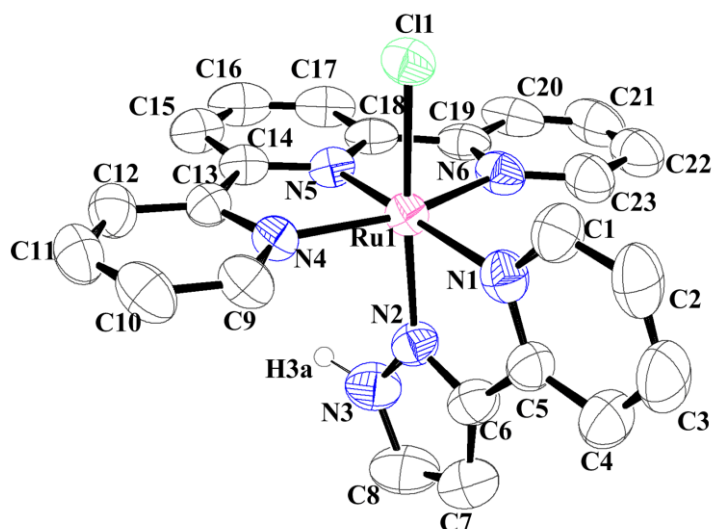


**Figure 2.** Plot and labelling scheme for **3a**.

The structure shows that the Ru metal center adopts an octahedral distorted type of coordination where the trpy ligand is bonded in a meridional manner and the pypz-H ligand acts in a didentate fashion. The sixth coordination site is occupied by the chlorido ligand. All bond distances and angles are within the expected values for this type of complexes.<sup>25</sup>

**Table 1.** Crystallographic data and details of the structure solution and refinement procedures for the X-ray diffraction of the complex **3a**.

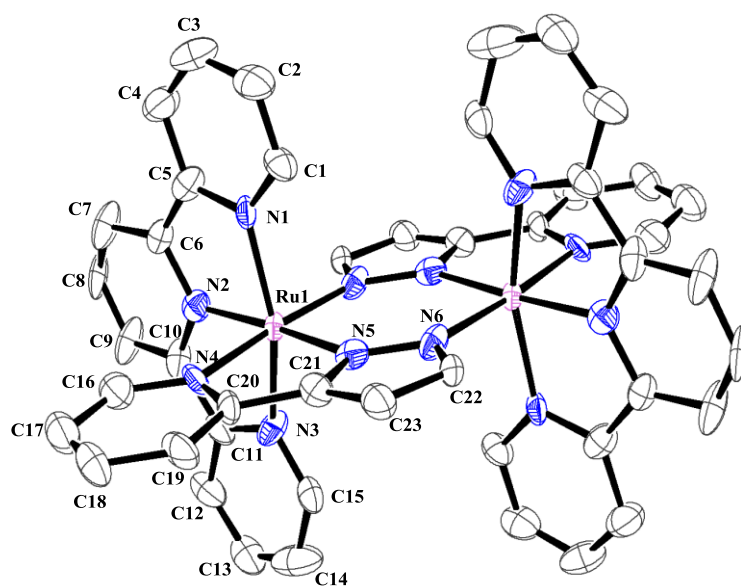
Empirical formula	C <sub>31</sub> H <sub>35</sub> Cl <sub>1</sub> N <sub>6</sub> O <sub>4</sub> F <sub>6</sub> P <sub>2</sub> Ru <sub>1</sub>
Formula weight	868.11
Crystal system	Triclinic
Space group	P-1
a[Å]	8.834(3)
b[Å]	14.292(4)
c[Å]	15.293(5)
α[°]	101.867(6)
β[°]	106.652(5)
γ[°]	95.095(5)
V [Å <sup>3</sup> ]	1787.8(9)
Formula Units/ cell	2
Temp. [K]	298(2)
ρ <sub>calc</sub> , [Mg/m <sup>-3</sup> ]	1.588
μ[mm <sup>-1</sup> ]	0.719
Final R indices, [I>2σ(I)]	R1 = 0.0722 wR2 = 0.2019
R indices [all data]	R1 = 0.0881 wR2 = 0.2221

**Table 2.** Selected bond lengths (Å) and angles (°) for **3a**.

<b>Ru(1)-N(1)</b>	2.103(5)	<b>N(1)-Ru(1)-N(4)</b>	104.61(17)	<b>N(2)-Ru(1)-Cl(1)</b>	170.82(12)
<b>Ru(1)-N(2)</b>	2.040(5)	<b>N(1)-Ru(1)-N(5)</b>	174.38(15)	<b>N(5)-Ru(1)-N(4)</b>	79.61(17)
<b>Ru(1)-N(4)</b>	2.076(4)	<b>N(1)-Ru(1)-N(6)</b>	95.99(18)	<b>N(5)-Ru(1)-N(6)</b>	79.78(18)
<b>Ru(1)-N(5)</b>	1.952(4)	<b>N(1)-Ru(1)-Cl(1)</b>	94.14(13)	<b>N(5)-Ru(1)-Cl(1)</b>	89.66(12)
<b>Ru(1)-N(6)</b>	2.081(4)	<b>N(2)-Ru(1)-N(4)</b>	91.48(16)	<b>N(4)-Ru(1)-N(6)</b>	159.38(18)
<b>Ru(1)-Cl(1)</b>	2.396(3)	<b>N(2)-Ru(1)-N(5)</b>	99.34(16)	<b>N(4)-Ru(1)-Cl(1)</b>	88.33(11)
<b>N(1)-Ru(1)-N(2)</b>	77.03(17)	<b>N(2)-Ru(1)-N(6)</b>	92.38(17)	<b>N(6)-Ru(1)-Cl(1)</b>	91.00(12)

The molecular structure of the dimeric ruthenium compound obtained together with **3b** during the synthetic process is shown in figure 3.

The structure shows two ruthenium atoms with octahedral distorted type of coordination where the trpy ligand is bonded in a meridional manner and the two deprotonated pyrazole rings of the pypz-H ligands bridging two ruthenium centers.

**Figure 3.** Plot and labelling scheme for dimeric ruthenium compound.

## 4.2 Spectroscopic properties

### 4.2.1 IR spectroscopy

Figures 4 and 5 show the IR spectra corresponding to the complexes **3a-3b**, and **4a**, respectively. All compounds show peaks around  $3090\text{ cm}^{-1}$ , that can be assigned to the  $\nu(\text{C-H})$  stretching corresponding to the polypyridylic ligands, also the IR spectra of compounds show peaks between  $1389\text{-}1412\text{ cm}^{-1}$  that can be assigned to the  $\nu(\text{C=N})$  stretching of the ligands. The peaks observed over  $1300\text{-}1100\text{ cm}^{-1}$  and at  $830\text{ cm}^{-1}$  can be assigned to the  $\delta(\text{C-H})$  in plane bends. Moreover, a double peak present in all the complexes at  $3600\text{-}3400\text{ cm}^{-1}$  corresponds to the  $\nu(\text{N-H})$  of the pyrazolic ligand. All spectra show a peak around  $845\text{ cm}^{-1}$  that can be assigned to the anion  $\text{PF}_6^-$ . In the case of the **4a** spectra (figure 5) it can be seen a new peak over  $3350\text{ cm}^{-1}$  which corresponds to the  $\nu(\text{O-H})$  stretching of the water coordinated to the metal.

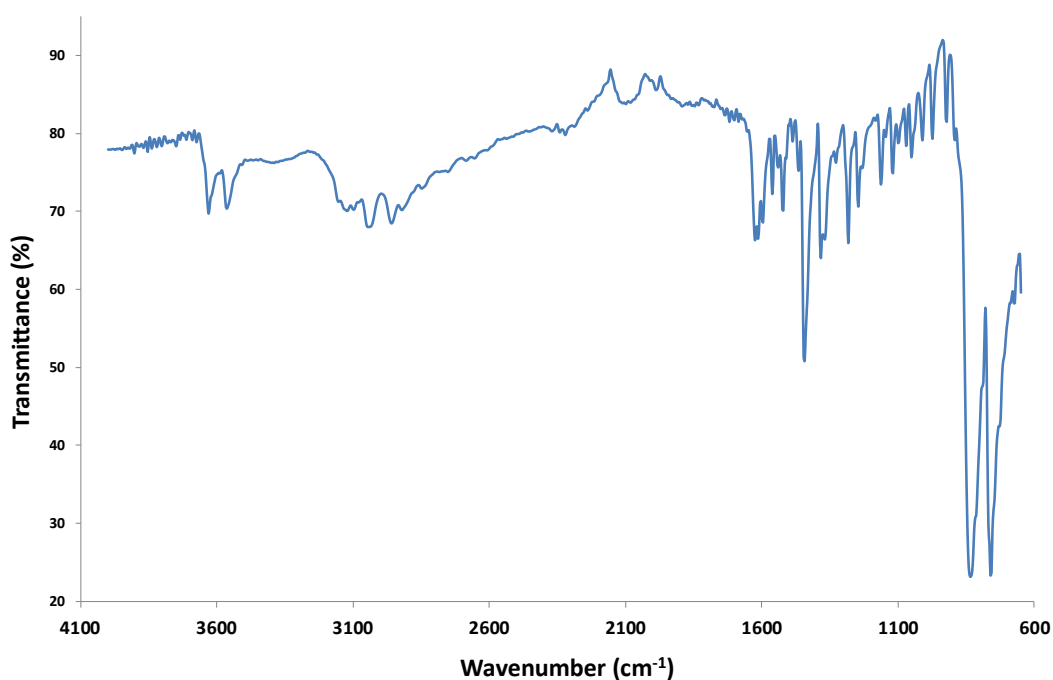


**Figure 4.** FTIR spectra of complex **3a**.

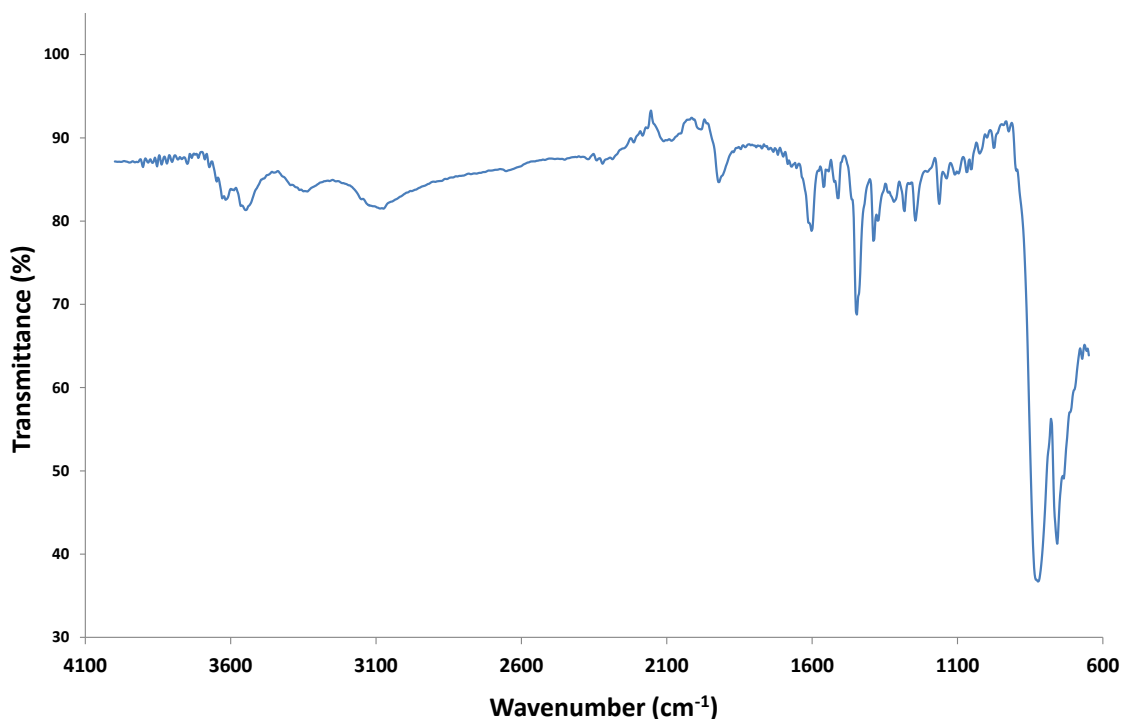
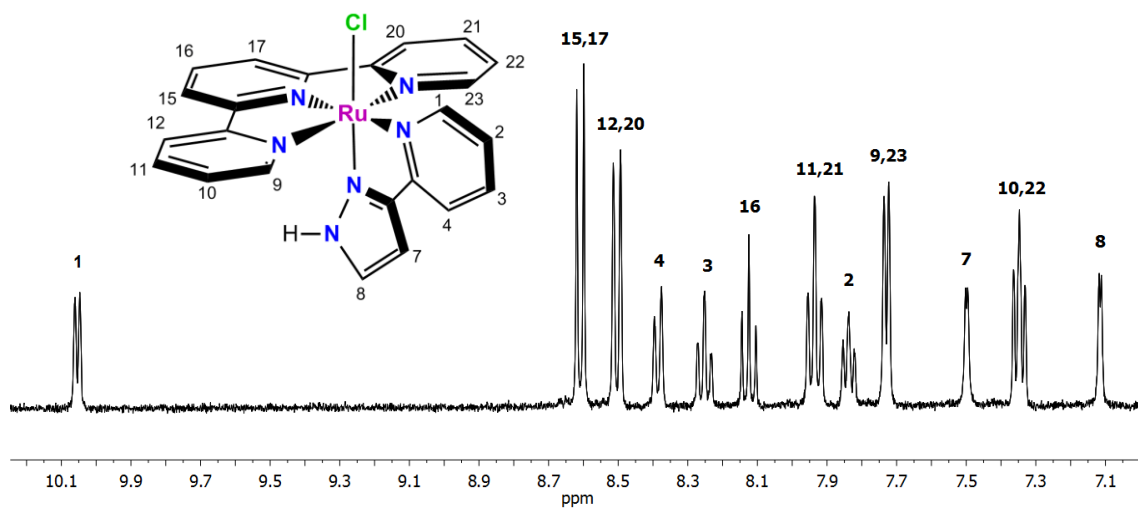
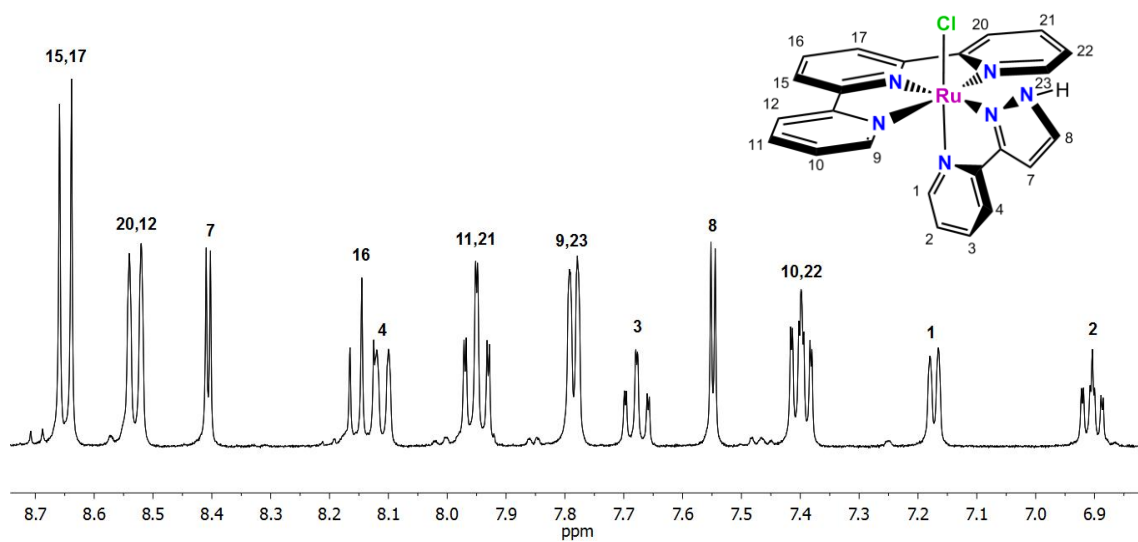
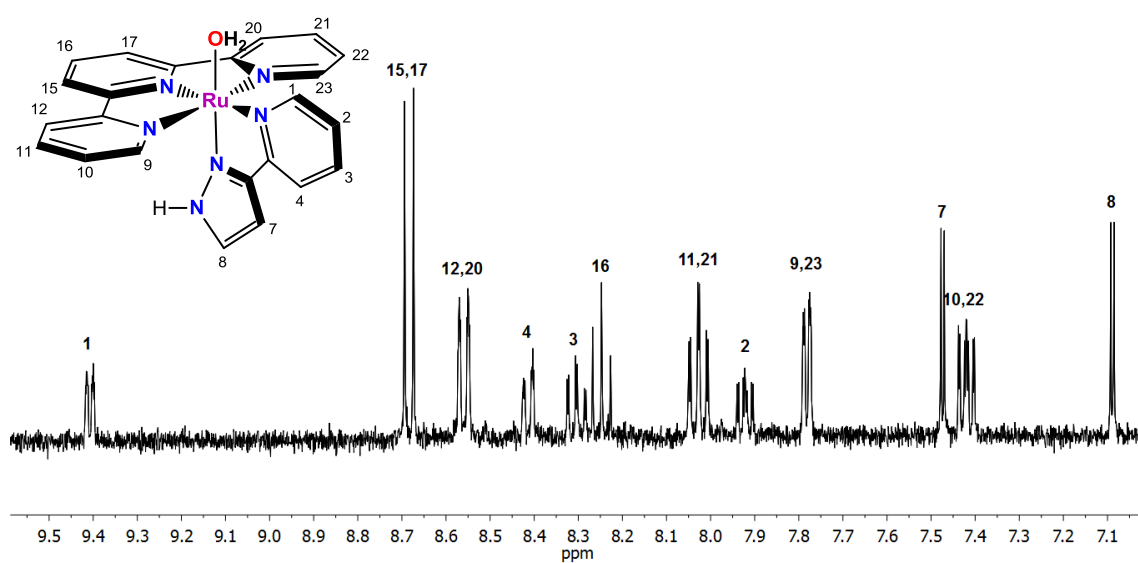


Figure 5. FTIR spectra of complex **4a**.

#### 4.2.2 NMR spectroscopy

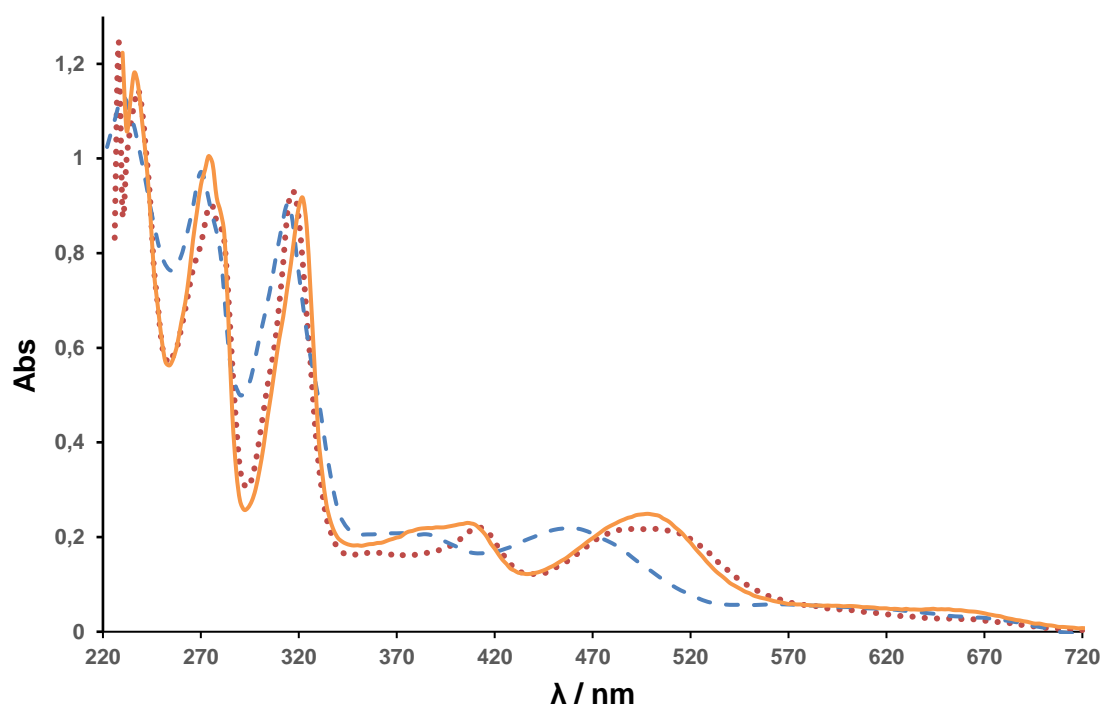
The one-dimensional (1D) NMR and two-dimensional (2D) spectra of complex **3a**, **3b** and **4a** were recorded in methanol- $d_4$  and are consistent with the solid-state structure of **3a**. Figure 6, 7 and 8 show the  $^1\text{H}$ -NMR spectra of complexes **3a**, **3b** and **4a**.  $^1\text{H}$ -NMR spectra exhibit one set of signals in the aromatic region associated with the presence of polypyridyl ligands. The most interesting feature of the spectra of complexes **3a** and **3b** (chloro-complexes) (figures 6, 7), respectively, is the deshielding effects exerted by the chlorido ligand over the H1, thus different chemical shifts of H1 are observed: 10,0 ppm for the *trans* isomer and 7.2 ppm for the *cis*. It is an evidence of the spatially close Cl ligand in the case of the *trans* isomer. For the Ru-OH $_2$  **4a** complex (figure 8) the deshielding effect of the OH $_2$  ligand over the H1, leads to a chemical shift of 9.4 ppm; this value is lower than the shift observed in the chloro-complex.



Figure 6.  $^1\text{H}$ -RMN spectrum of complex 3a.Figure 7.  $^1\text{H}$ -RMN spectrum of complex 3b.Figure 8.  $^1\text{H}$ -RMN spectra of complex 4a.

### 4.2.3 UV-Vis spectroscopy

The UV-Vis spectra of complexes **3a**, **3b** and **4a** are displayed in Figure 9 whereas their main features are presented in the experimental section. The complexes exhibit ligand based  $\pi$ - $\pi^*$  bands below 350 nm and relatively intense bands above 350 nm assigned mainly to  $d\pi$ - $\pi^*$  transitions due to a series of MLCT transitions.<sup>26</sup> For the Ru-Cl complexes the MLCT bands are shifted to the red with regard to the Ru-OH<sub>2</sub> due to the relative destabilization of the  $d\pi$ (Ru) levels provoked by the chloro ligand (see Figure 9). A similar MLCT value are observed for other complexes described in the literature.<sup>27</sup>



**Figure 9.** UV/Vis spectra of **3a** (solid line), **3b** (dotted dashed line) in DCM and **4a** (dashed line) in phosphate buffer (pH=7).

### 4.3 Electrochemical properties

The redox properties of the Ru-Cl and aqua complexes described in the present work were investigated by means of cyclic voltammetry (CV) and differential pulse voltammetry (DPV) and are summarized in Table 3. Figure 10 shows the CVs for **3a** and **3b**, and figure 11 shows the DPV of **4a**.

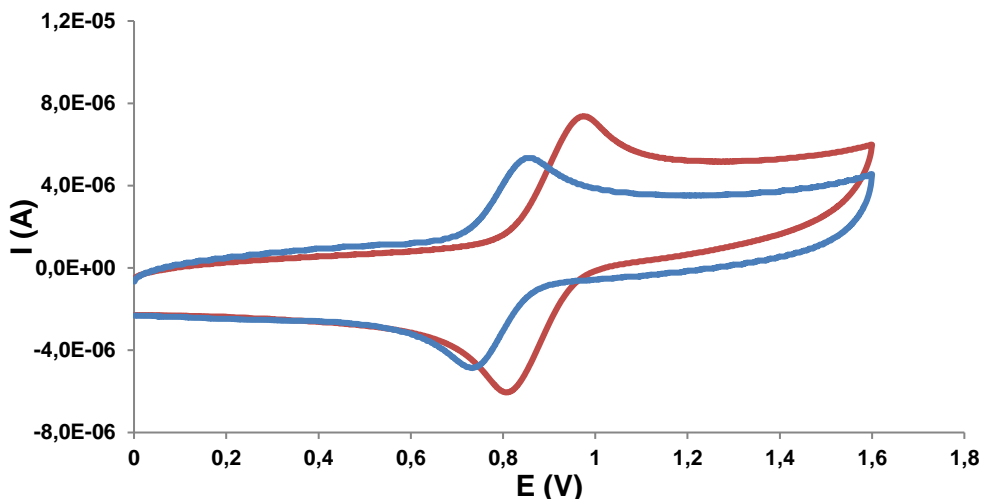


**Figure 10.** CV for complex **3a** (blue) and **3b** (red) exhibits a reversible Ru(III)/Ru(II) redox wave at  $E_{1/2} = 0.80$  V and  $E_{1/2} = 0.88$  V respectively. Both registered in  $\text{CH}_2\text{Cl}_2$  with SCE as the reference electrode.

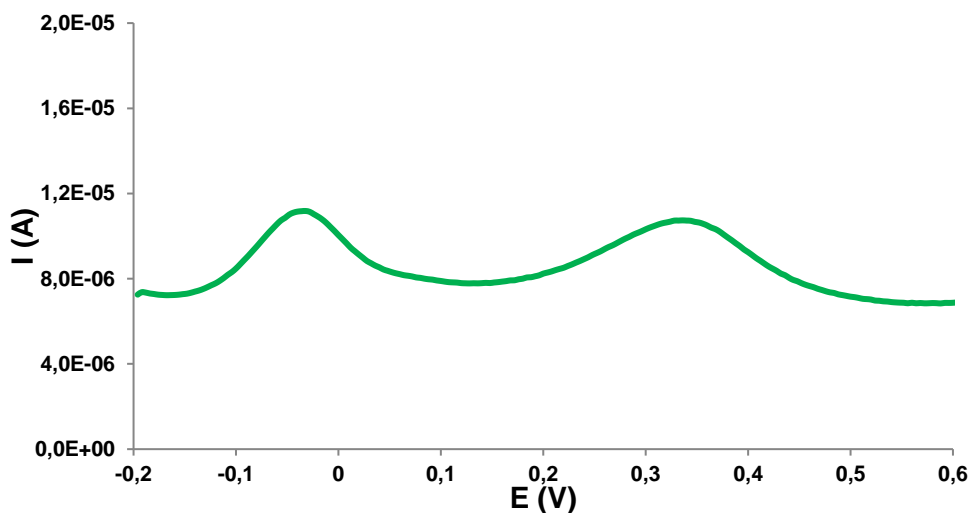


**Figure 11.** DPV for complex **4a** exhibits a Ru(III)/Ru(II) at  $E_{1/2} = 0.03$  V and a Ru(IV)/Ru(III) at  $E_{1/2} = 0.34$  V registered in phosphate buffer (pH=11.8) with SCE as the reference electrode. The redox potentials for the Ru-aqua complexes are pH dependent (1) due to the capacity of the mentioned aqua ligand to lose protons as has been shown in equations (2-7).

$$E_{1/2} = E^{\circ}_{1/2} - 0.059 (m/n) \text{ pH} \quad (1)$$

- $E_{1/2}$ : half wave redox potential at a given pH  
 $E^{\circ}_{1/2}$ : half wave redox potential at standard conditions  
 m: number of transferred protons  
 n: number of transferred electrons

**Equation 1.** Relation between potential and pH in the Nernst equation. The complete thermodynamic information regarding the Ru-aqua type of complex can be extracted from the Pourbaix diagrams, exhibited in Figure 12 for **4a**.

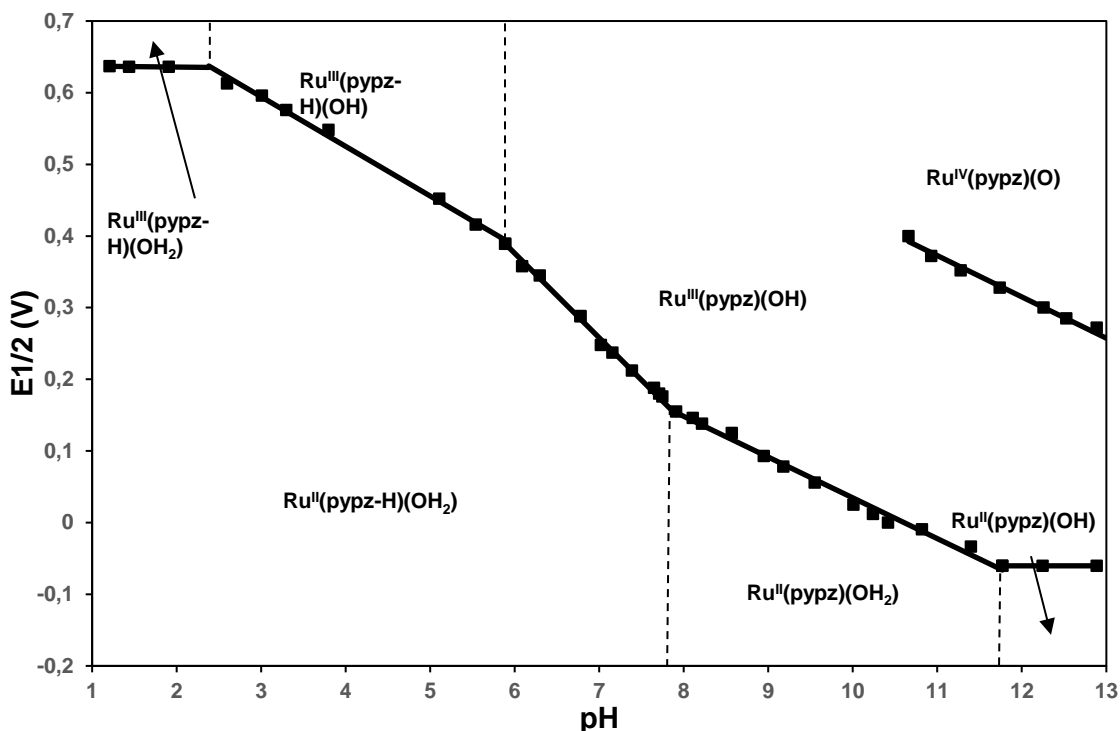
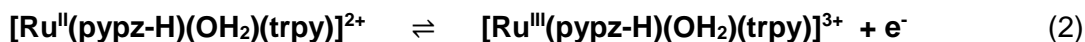
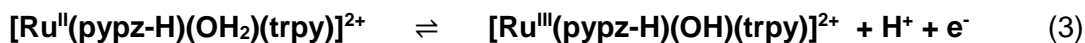


**Figure 12.** Pourbaix diagram for complex **4a**. The stability zones and the proton composition for the different redox species are indicated. The pKa of each species are represented with a dashed vertical line.

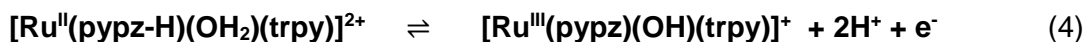
Under strong acid conditions,  $\text{pH} < 2.2$ , the potential is not dependent from de pH and only one chemically reversible wave is observed at  $E_{1/2}=0.64$  V corresponding to the process represented according to the Equation 2:



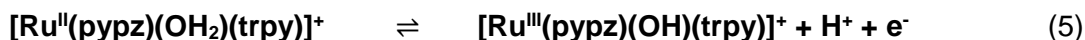
Within the pH range 2.2-6.0 approximately, the potential corresponding to the couple Ru(III/II) decrease 69 mV for pH unit. This variation according to the Nernst prediction (Equation 1) is consistent with a process that exchanged one proton and one electron, with a theoretical slope of 59 mV for pH unit (see Equation 3):



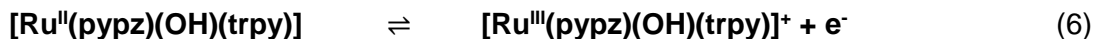
Within the pH range 6.0-7.9, the potential decrease 118 mV for pH unit, which indicate that two protons and one electron are exchanged (see Equation 4):



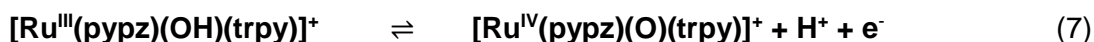
Within the pH range 7.9-11.8 approximately, the potential decrease 57 mV for pH unit. This variation is consistent with a process that exchanged one proton and one electron, (see Equation 5).



Under strong basic conditions, pH >10.8, the wave potential is not dependent from de pH and the process can be represented according to the Equation 6:



A second wave is observed over pH>10.5 it corresponds to the redox couple Ru(IV/III), where the potential decreases 58 mV for pH unit,



The changes in the slope correspond to the pKa values of the Ru(II) and Ru(III) species, respectively, and are indicated by the vertical lines in each case, The acid-base equilibria are displayed below:

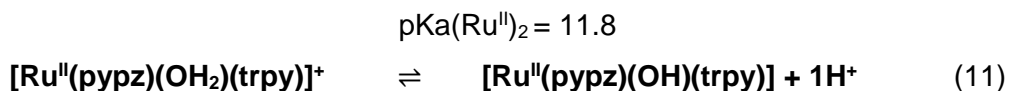
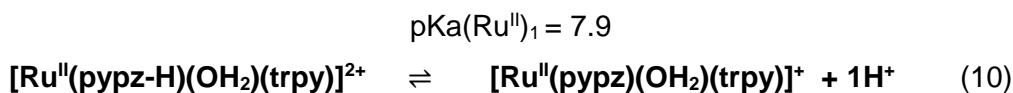
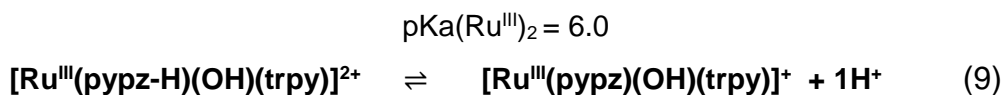
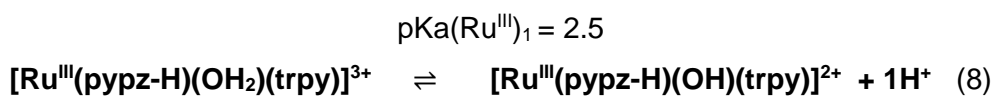


**Table 3.** pKa and electrochemical data (pH = 7,  $E_{1/2}$  in V vs SCE) for aqua complexes described in this work and others for purposes of comparison.

entry	compound	$E_{1/2}$ (III/II)	$E_{1/2}$ (IV/III)	$\Delta E^a$	pK <sub>a</sub> (II)	pK <sub>a</sub> (III)	ref
1	<b>4a</b>	0.26	0.65	390	11.8(7.9)	2.5(6)	<i>b</i>
2	<i>trans</i> -[Ru(trpy)(pypz-Me)(OH <sub>2</sub> )] <sup>2+</sup>	0.39	0.57	180	10.1	0.95	25b
3	[Ru(trpy)(bpy)(OH <sub>2</sub> )] <sup>2+</sup>	0.42	0.62	130	9.7	1.7	27a
4	[Ru(trpy)(acac)(OH <sub>2</sub> )] <sup>2+</sup>	0.19	0.56	370	11.2	5.2	27b

<sup>a</sup> $\Delta E = E_{1/2}(IV/III) - E_{1/2}(III/II)$  in mV. <sup>b</sup>This work.

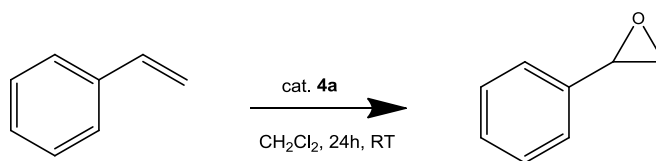
Table 3 shows the comparison of the redox potential of our Ru-OH<sub>2</sub> complex with those previously reported in the literature.<sup>25b,28</sup> The redox potential of the couple Ru(III/II) of **4a** is lower than the analogous *trans*-[Ru<sup>II</sup>(trpy)(pypz-Me)(OH<sub>2</sub>)]<sup>2+</sup>, which is in accordance with the strong electron-donor character of the pypz-H ligand. This fact is also corroborated by the values of  $\Delta E$  that in the case of [Ru(trpy)(bpy)(H<sub>2</sub>O)]<sup>2+</sup> complex at pH=7 and *trans*-[Ru(trpy)(pypz-Me)(OH<sub>2</sub>)]<sup>2+</sup> both possess a  $\Delta E = 130$  mV and 180 mV, respectively. The substitution of bpy or pypz-Me ligands by strong  $\sigma$ -donor ligands such as acetylacetonate (acac) produces a stabilization of the Ru(IV) and Ru(III) oxidation states with regard to the bpy or pypz-Me, as consequence of the strong decrease of the III/II couple while the IV/III is much less affected  $E_{1/2}(IV/III)=0.56$  V,  $E_{1/2}(III/II)=0.19$  V,  $\Delta E = 370$  mV indicating that the oxidation states IV and III are affected in a relatively similar manner by the (acac) ligand. A similar phenomenon is also observed for complex **4a** (pH=7):  $E_{1/2}(IV/III)=0.65$  V,  $E_{1/2}(III/II)=0.29$  V,  $\Delta E=360$  mV) showing that the anionic nature of the (pypz<sup>-</sup>) ligand also produces a strong stabilization of oxidation states IV and III. Complex **4a** has higher pka<sub>4</sub> (11.8) than complex in entry 2, (10.1), this less acidic character for **4a** is again in accordance with the anionic nature of the pypz-H, ligand that is deprotonated to this pH value.

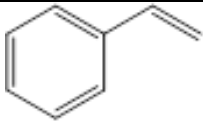
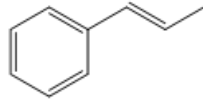
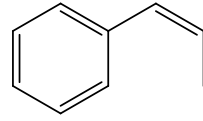
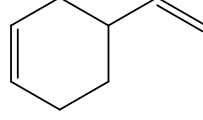
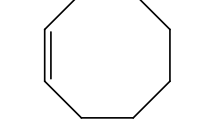
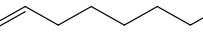
#### 4.4 Catalytic epoxidation reactions

This process has been assessed using different alkenes as substrates. The reaction has been performed at room temperature for 24 hours using PhI(OAc)<sub>2</sub> as the oxidant, a catalyst/substrate/oxidant ratio of 1:100:200 and CH<sub>2</sub>Cl<sub>2</sub> as solvent. No epoxidation occurred in the absence of catalyst. The remaining substrate has been quantified through GC analysis and employing biphenyl as an internal standard.

In Table 5 the catalytic results are shown.

**Table 5.** Ru-catalyzed alkene epoxidation.<sup>a</sup> Conversion (conv) and selectivity (sel) values are given in %.



Substrate	Conv	Sel <sup>b</sup>
	69	>99
	86	>82
	90 (78/22) <sup>c</sup>	>99
	>99 (100/0) <sup>d</sup>	>99
	94	>99
	66	>99

<sup>a</sup>Oxidation conditions: **4a**:subs:PhI(OAc)<sub>2</sub> (catalyst/substrate/oxidant) ratio of 1:100:200 in CH<sub>2</sub>Cl<sub>2</sub>, 24 h at RT. <sup>b</sup>Selectivity for epoxide (sel): [Yield/conversion]x100. <sup>c</sup>Ratio [% cis epoxide / % trans epoxide]. <sup>d</sup>Ratio [% ring epoxide/ % vinyl epoxide].

As can be observed in Table 5, in general high conversion and selectivity values for the corresponding epoxides (with benzaldehyde identified as main byproduct) are obtained for all the substrates tested.

The activity of catalyst with regard to the epoxidation of *cis*- $\beta$ -methylstyrene shows 78% of *cis*-epoxide and 22% of *trans*-epoxide; this fact is caused by the isomerization to the most thermodynamic stable isomer *trans*. It is interesting to compare the activity of our catalyst with regard to *trans*-[Ru(trpy)(pypz-Me)(OH<sub>2</sub>)]<sup>2+</sup>,<sup>25b</sup> which the isomerization to the *trans*-epoxide is inexistent, This fact could be in agreement with the high stability of Ru(III) in our complex and that the existence of a radical mechanism could take place.

By report to 4-vinylcyclohexene, the catalyst showed preference towards the ring epoxidation, this is in agreement with the existence of electrophilic catalytic species since the more electron-rich aliphatic olefin is oxidized faster.

Finally, with cyclooctene as substrate it has been obtained higher conversion values than with 1-octene. This is in accordance with the lower reactivity towards unactivated monosubstituted alkenes.

## CHAPTER 5. CONCLUSIONS

1. Two new ruthenium complexes containing the tridentate trpy and the nonsymmetric didentate pypz-H ligands, *cis* and *trans*-[Ru<sup>II</sup>Cl(trpy)(pypz-H)](PF<sub>6</sub>) **3b** and **3a** and *trans*-[Ru<sup>II</sup>(trpy)(pypz-H)(OH<sub>2</sub>)](PF<sub>6</sub>)<sub>2</sub> **4a**, have been synthesized and thoroughly characterized by structural, analytical and spectroscopic techniques.
2. In the case of the chlorido complex, a mixture of two isomers (*cis* and *trans*) were obtained and were separated. The crystal structure of the *trans* isomer has been solved through X-ray diffraction analysis, showing a distorted octahedral environment for the Ru metal center. However, the *cis* isomer is obtained in low yields and together with side products like the dimer specie shown in the x-Ray structure.
3. The 2 isomers *cis* and *trans* of the Ru complex [Ru<sup>II</sup>Cl(pypz-H)(trpy)](PF<sub>6</sub>) **3b** and **3a** were obtained with a ratio of 4:1 being the *trans* isomer the most favored one, due to the formation of an hydrogen bond between the chloride ligand and a proton of the pyridine inside the pypz-H ligand.
4. The aqua-complex **4a** and **4b** were easily obtained after refluxing the chlorido complex **3a** and **3b** in water and in the presence of Ag<sup>+</sup> as precipitating reagent.



5. All the complexes have been thoroughly characterized spectroscopically and electrochemically. The spectroscopic  $^1\text{H-NMR}$  analysis are consistent with the presence of the corresponding compounds and in the case of **3a** complex exhibit a strong downfield shift for the pyridylic proton next to the chloride ligand.
6. For the electrochemical data it can be seen that the **3a** isomer have a lower redox potential than **3b**, (80 mV vs 88 mV); this fact can be rationalized in terms of the hydrogen interaction with the Cl ligand, stabilizing the  $\text{Ru}^{\text{III}}$  oxidation state in the case of the trans- isomer, which has a stronger H-Cl interaction, and thus decreases the  $\text{Ru}^{\text{III}}/\text{Ru}^{\text{II}}$  redox potential.
7. **4a** complex displays two pH-dependent redox processes corresponding to the  $\text{Ru}^{\text{IV}}/\text{Ru}^{\text{III}}$  and  $\text{Ru}^{\text{III}}/\text{Ru}^{\text{II}}$  redox pairs. The Pourbaix diagram indicates that two deprotonation processes can take place, corresponding to the deprotonation of the pypz-H and aqua ligands.
8. Compound **4a** was tested in the epoxidation of different alkenes, showing good conversion and selectivity values, in the case *cis*- $\beta$ -methylstyrene shows a certain isomerization to the *trans*-epoxide. This behavior is consistent with the higher stabilization of the  $\text{Ru}(\text{IV})$  and  $\text{Ru}(\text{III})$  oxidation states with regard to similar complexes containing bpy or pypz-Me ligands.

## CHAPTER 6. BIBLIOGRAPHY

- <sup>1</sup> Qu, P.; Thompson, D. W.; Meyer, G. J. *Langmuir*, **2000**, *16*, 4662.
- <sup>2</sup> Murahashi, S.I.; Takaya, H.; Naota, T. *Pure Appl. Chem.* **2002**, *74*, 19. Rodríguez M.; Romero, I.; Llobet, A.; Deronzier, A.; Biner, M.; Parella, T.; Stoeckli-Evans H. *Inorg. Chem.* **2001**, *40*, 4150.
- <sup>3</sup> Nikolau, S.; Toma, H.E. *J. Chem. Soc., Dalton Trans.* **2002**, 352. Rodríguez, M.; Romero, I.; Llobet, A.; Collomb-Dunand-Sauthier, M. N.; Deronzier, A.; Parella, T.; Stoeckli-Evans, H. *J. Chem. Soc., Dalton Trans.* **2000**, 1689.
- <sup>4</sup> Clarke, M. J. *Coord. Chem. Rev.* **2003**, *236*, 209.
- <sup>5</sup> Balzani, V.; Bergamini, G.; Marchioni, F.; Ceroni, P. *Coord. Chem. Rev.* **2006**, *250*, 1254.
- <sup>6</sup> Zhang, S.; Ding, Y.; Wei, H. *Molecules*. **2014**, *19*, 11933.
- <sup>7</sup> Coe, B. J. *Coord. Chem. Rev.* **2013**, *257*, 1438. Yoshida, J.; Watanabe, G.; Kakizawa, K.; Kawabata, Y.; Yuge, H. *Inorg. Chem.* **2014**, *52*, 11042.
- <sup>8</sup> Zhang, S.; Ding, Y.; Wei, H. *Molecules* **2014**, *19*, 11933.
- <sup>9</sup> a) Serrano, I.; López, M. I.; Ferrer, I.; Poater, A.; Parella, T.; Fontrodona, X.; Solà, M.; Llobet, A.; Rodríguez, M.; Romero, I. *Inorg. Chem.* **2011**, *50*, 6044-6054. b) Dakkach, M.; Fontrodona, X.; Parella, T.; Atlamsani, A.; Romero, I.; Rodríguez, M. *Advanced Synthesis & Catalysis*. **2011**, *353*, 231-238.
- <sup>10</sup> Alstreen-Acebedo, J. H.; Brennaman, M.K.; Meyer T.U. *Inorg. Chem.* **2005**, *44*, 6802-6872. Hammarstrom, L.; Sun, L.C.; Akemark, B.; Stryring, S. *Catal. Today*. **2000**, *58*, 57-69.
- <sup>11</sup> Barigelletti, F.; Flamigni, L. *Chem. Soc. Rev.* **2000**, *29*, 1. Yin, J.-F.; Velayudham, M.; Bhattacharya, D.; Lin, H.-C.; Lu, K.-L. *Coord. Chem. Rev.* **2012**, *256*, 3008.
- <sup>12</sup> Jiang, C.W.; Chao, H.; Hong, X. L.; Li, H.; Mei, W. J.; Ji, L. N. *Inorg. Chem. Commun.* **2003**, *6*, 773-775.
- <sup>13</sup> Costentin, C.; Robert, M.; Saveant, J.-M. *Chem. Rev.* **2010**, *110*, PR1-PR40.
- <sup>14</sup> Banu, A.; Stan, R.; Matondo, H.; Perez, E.; Rico-Lattes, I.; Lattes, A. *C. R. Chim.* **2005**, *8*, 853.
- <sup>15</sup> Upjohn, J. *Am. Chem. Soc.* **1956**, 6213.
- <sup>16</sup> a) Dakkach, M.; Atlamsani, A.; Parella, T.; Fontrodona, X.; Romero, I.; Rodríguez, M. *Inorg. Chem.* **2013**, *52*, 5077. b) Aguiló, J.; Francàs, L.; Bofill, R.; Gil-Sepulcre, M.; García-Antón, J.; Poater, A.; Llobet, A.; Escriche, L.; Meyer, F.; Sala, X. *Inorg. Chem.* **2015**, *54*, 6782. c) Dakkach, M.; Atlamsani, A.; Parella, T.; Fontrodona, X.; Romero, I.; Rodríguez, M. *Adv. Synth. Catal.* **2011**, *353*, 231. d) Barf, G. A.; Sheldon, R. A. *J. Mol. Catal. A: Chem.* **1995**, *98*, 143.
- <sup>17</sup> a) Dhuri, S. N.; Cho, K.-B.; Lee, Y.-M.; Shin, S. Y.; Kim, J. H.; Mandal, D.; Shaik, S.; Nam, W. *J. Am. Chem. Soc.* **2015**, *137*, 8623. b) Masllorens, E.; Rodríguez, M.; Romero, I.; Roglans, A.; Parella, T.; Benet-Buchholz, J.; Poyatos, M.; Llobet, A. *J. Am. Chem. Soc.*, **2006**, *128*, 5306.
- <sup>18</sup> Bruker Advanced X-ray Solutions. SMART: Version 5.631, **1997-2002**.
- <sup>19</sup> Bruker Advanced X-ray Solutions. SAINT +, Version 6.36A, **2001**.
- <sup>20</sup> Sheldrick, G. M. *Empirical Absorption Correction Program*, Universität Göttingen, **1996**.
- <sup>21</sup> Sheldrick, G. M. *Program for Crystal Structure Refinement*, Universität Göttingen, **1997**. SHELXT- SHELXL-2014/7 (Sheldrick, 2014).
- <sup>22</sup> Brunner, H.; Scheck, T. *Chem. Ber.* **1992**, *124*, 701.
- <sup>23</sup> Evans, I. P.; Spencer, A.; Wilkinson, J.J.; *J. Chem. Soc., Dalton Trans.* **1973**, *2*, 204.
- <sup>24</sup> Ferrer, I.; Rich, J.; Fontrodona, X.; Rodríguez, M.; Romero, I. *Dalton Trans.* **2013**, *42*, 13461.
- <sup>25</sup> a) Sens, C.; Rodríguez, M.; Romero, I.; Llobet, A.; Parella, T.; Benet-Buchholz, J. *Inorg. Chem.* **2003**, *42*, 8385-8394. b) Dakkach, M.; López, M. I.; Romero, I.; Rodríguez, M.; Atlamsani, A.; Parella, T.; Fontrodona, X.; Llobet, A. *Inorg. Chem.* **2010**, *49*, 7072-7079.
- <sup>26</sup> Balzani, V.; Juris, A.; Veturi, M. *Chem. Rev.* **1996**, *96*, 759.
- <sup>27</sup> Roeser, S.; Farràs, P.; Bozoglian, F.; Martínez-Belmonte, M.; Benet-Buchholz, J.; Llobet, A. *ChemSusChem* **2011**, *4*, 197-207.
- <sup>28</sup> a) Binstead, R. A.; Meyer, T. J. *J. Am. Chem. Soc.* **1987**, *109*, 3287-3297. b) Bessel, C. A.; Leising, R. A.; Takeuchi, K. J. *J. Chem. Soc.; Chem. Commun.* **1991**, 883-835.